Int. J. Heat Mass Transfer. Vol. 10, pp. 1389–1411. Pergamon Press Ltd. 1967. Printed in Great Britain

A FINITE-DIFFERENCE PROCEDURE FOR SOLVING THE EQUATIONS OF THE TWO-DIMENSIONAL BOUNDARY LAYER

S. V. PATANKAR† and D. B. SPALDING
Mechanical Engineering Department, Imperial College, London

(*Received* 27 *February* 1967)

Abstract—A general, implicit, numerical, marching procedure is presented for the solution of parabolic partial differential equations, with special reference to those of the boundary layer. The main novelty lies in the choice of a grid which adjusts its width so as to conform to the thickness of the layer in which significant property gradients are present. The non-dimensional stream function is employed as the independent variable across the layer.

The capabilities of the method are demonstrated by application to: the heated flat plate in a high-Mach-number laminar stream; the axi-symmetrical turbulent jet in moving and stagnant surroundings; and the radial turbulent wall jet.

NOMENCLATURE

(The number in the parentheses denotes the equation of first mention.)

a, a group of symbols in the convection term (3.1.1);
A, a coefficient in the difference equation (3.2.3);
b, a group of symbols in the convection term (3.1.1);
B, a coefficient in the difference equation (3.2.3);
c, a group of symbols in the diffusion term (3.1.1);
$\bar{c}_f$, mean skin-friction coefficient;
C, a quantity in the difference equation (3.2.3);
d, diameter of the jet nozzle (4.2.1);
D, a coefficient in the difference equation for V_1 (3.2.4);
D_k, dissipation of the turbulent kinetic energy (2.1.9);
E, a coefficient in the transformed difference equation (3.3.7);
f, a fraction between zero and unity;
F, a quantity in the transformed difference equation (3.3.7);
g_1, g_2, g_3, g_4, coefficients in the difference form of the convection term (3.2.2);
G_1, $\equiv \rho V_1$ (2.1.2);
G_2, $\equiv \rho V_2$ (2.1.2);
G_θ, $\equiv \rho V_\theta$ (2.1.4);
h, specific enthalpy (2.2.6);
$\tilde{h}$, stagnation enthalpy (2.1.7);
H, a coefficient in the transformed difference equation (3.3.7);
J, diffusional flux (3.4.1);
k, mean kinetic energy of the fluctuating motion per unit mass (2.1.7);
l_1, l_2, the length scales in direction 1 and 2 (2.1.1);
l_m, mixing length (2.2.3);
l_k, length scale associated with k (2.2.4);
L, a coefficient in the transformed difference equation (3.3.11);
m_j, mass fraction of a chemical species j (2.1.8);

† Present address: Mechanical Engineering Department, Indian Institute of Technology, Kanpur, India.

M, a quantity in the transformed difference equation (3.3.11);
N, number of strips across the layer;
p, pressure (2.1.4);
P, a coefficient in the transformed difference equation (3.3.2);
Q, a quantity in the transformed difference equation (3.3.2);
r, radius, distance from the axis of symmetry (2.1.2);
$r_{\frac{1}{2}}$, the radius at which the velocity is one-half of the centre-line velocity;
R, a coefficient in the transformed difference equation (3.3.5);
Re, Reynolds number, $(\rho_G u_G x/\mu_G)$;
R_j, rate of generation of the chemical species j (2.1.8);
s, distance along the $\xi_1 \sim \xi_2$ plane (2.1.1);
S_ϕ, Stanton-number function for ϕ (2.3.1);
St, the Stanton number;
T, absolute temperature (4.1.1);
u, velocity in longitudinal direction (4.2.1);
u^+, dimensionless velocity $[u/\sqrt{(\tau_S/\rho)}]$ (4.3.2);
u_c, velocity at the wall-jet slot;
$u_{\max}$, maximum velocity in the wall-jet profile;
V_1, velocity in direction 1 (2.1.3);
V_2, velocity in direction 2 (2.1.3);
V_r, velocity in radial direction (2.1.6);
V_θ, velocity in direction θ (2.1.4);
x, longitudinal distance (4.2.1);
y, distance across the layer;
y^+, dimensionless distance $(y\sqrt{(\tau_S\rho)}/\mu)$ (4.3.2);
$y_{\frac{1}{2}}$, half-value thickness of the wall jet;
y_c, thickness of the wall-jet slot;
y_l, characteristic thickness of the layer used to calculate the mixing length (4.3.1).

Greek symbols

β, the angle made by direction 1 with the symmetry axis (2.1.4);
γ, the ratio of specific heats;
κ, a constant in the mixing-length formula (4.3.1);
λ_G, a constant in the the mixing-length formula (4.3.1);
μ, laminar viscosity (2.3.1);
$\mu_{1,\text{eff}}$, effective viscosity in direction 1 (2.1.4);
$\mu_{\theta,\text{eff}}$, effective viscosity in direction θ;
ξ_1, coordinate in direction 1 (2.1.1);
ξ_2, coordinate in direction 2 (2.1.1);
ρ, fluid density (2.1.3);
σ, laminar Prandtl or Schmidt number (2.3.1);
$\sigma_{h,\text{eff}}$, effective Prandtl number (2.1.7);
$\sigma_{j,\text{eff}}$, effective Schmidt number for species j (2.1.8);
$\sigma_{k,\text{eff}}$, effective Prandtl number for the diffusion of k (2.1.7);
$\sigma_{\theta,\text{eff}}$, $\equiv \mu_{1,\text{eff}}/\mu_{\theta,\text{eff}}$ (2.1.6);
τ_S, shear stress at the wall;
ϕ, a typical dependent variable (2.1.10);
ϕ^*, a predetermined value of ϕ used in the grid-control formula (3.6.3);
Φ, a term representing generation of ϕ in the typical equation (2.1.10);
ψ, a stream function (2.1.3);
ω, dimensionless steam function, coordinate in direction 2 (2.1.11).

Subscripts

D, the downstream point on a portion of the grid;
$D+, D-$, points near to and at the same value of ξ_1 as D;
E, the external boundary of the layer;
G, a free-stream boundary;
$G-$, a point within the layer, near to and at the same value of ξ_1 as G;
I, the internal boundary of the layer;
S, a wall boundary;
$S+$, a point within the layer, near to and at the same value of ξ_1 as S;
U, the upstream point on a portion of the grid;
$U+, U-$, points near to and at the same value of ξ_1 as U;

0, the initial line; jet-nozzle condition;
1, the coordinate direction 1;
2, the coordinate direction 2;
θ, the direction perpendicular to the radius and in a plane normal to the symmetry axis;
ϕ, pertaining to the dependent variable ϕ.

1. INTRODUCTION

1.1. *The problem considered*

HEAT-, mass- and momentum-transfer in steadily flowing media are governed by elliptic differential equations. Because these are difficult to solve, the elliptic equations are often, and legitimately, truncated to a parabolic form; these truncated equations are the boundary-layer equations.

The present paper provides a new method of solving these equations. That a new method may be desirable is shown by the fact that existing methods are still not widely used; they are either too expensive to operate, too difficult to adapt to particular problems, or too prone to failures and inaccuracies. For this reason many authors, including the present ones, have put forward approximate procedures of calculation [1], in which only a few, integral, forms of the partial differential equations are solved; but these too have their shortcomings.

The solution procedures which are simplest in concept are those of the numerical, finite-difference type. Many variants have been suggested and employed successfully; but they are open to the above-mentioned objections. The new method is also of the finite-difference variety; but it embodies special devices for reducing the computation time, without loss of accuracy, and for bringing many types of problems within the scope of a single computer programme.

1.2. *Some remarks on earlier finite-difference methods*

Classification. Finite-difference procedures for parabolic equations can be distinguished according to the co-ordinate systems which they employ, and according to whether they are "explicit" or "implicit" in character.

Choice of finite-difference formula. For unsteady-heat-conduction problems, the explicit methods are typified by the Binder–Schmidt procedure [2], whereas the implicit methods are typified by that of Crank and Nicholson [3]. The advantages and disadvantages are well known. Explicit methods involve only simple arithmetic; but the time interval must not exceed a fixed proportion of the square of the space interval divided by the thermal diffusivity. Implicit methods involve much more arithmetic per time interval, because simultaneous equations appear, requiring solution by matrix-inversion or successive-substitution techniques; on the other hand, they are free from any limitation on the size of the time interval.

Whether explicit or implicit methods are preferable for heat-conduction problems remains a matter of opinion. For the problems which arise in boundary-layer theory, on the other hand, the superiority of the implicit method is becoming widely recognised. This superiority results from the fact that the explicit method here has an upper limit on the distance interval in the stream direction; and this limit is directly proportional to the fluid velocity. Since this velocity may become very small near a wall, very small distance steps must be taken; the implicit method, which is free from this restriction, therefore requires much less computing time than the explicit one.

Although the implicit method necessitates matrix inversion, the matrix is a simple one; so inversion may be achieved by way of recurrence relations. The procedure of Pashkonov [4] is typical; it employs the Crank–Nicholson form of the finite-difference formulae, and has been developed for predicting the flow in laminar boundary layers.

Choice of coordinate system. Figure 1 illustrates a typical choice of coordinate grid, and enables its disadvantage to be clearly observed. The $x \sim y$ grid is rectangular, and coincides

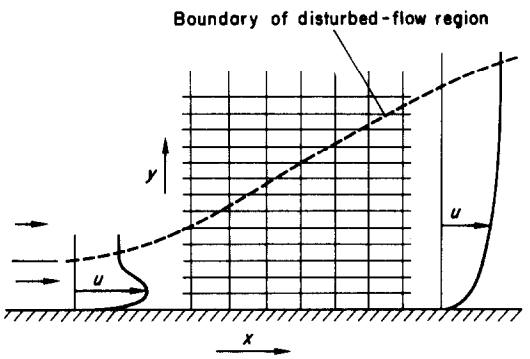

FIG. 1. The growth of a wall jet into a surrounding stream. The sketch shows how the region of disturbed flow widens in the downstream direction.

at one edge with the wall which bounds the region of interest. The other boundary of this region, shown dotted on the diagram, extends obliquely across the grid. Now, to achieve accuracy, a certain minimum number of grid points should be contained at the upstream end within the thickness of the layer. Obviously therefore, sufficient accuracy in the upstream region is purchased at the expense of an excessively fine grid for the downstream region. So a rectangular grid is likely to be inefficient; computations made with its aid are unnecessarily expensive.

Although several means have been proposed for solving this difficulty, none is both neat and generally applicable. There is therefore a need for a general coordinate system which allows the requirements of accuracy to be reconciled with those of elegance and of computational efficiency.

1.3. *Outline of the present contribution*

The calculation procedure that is described below is of the "implicit" variety. The scheme differs slightly from that of Crank and Nicholson; but, like that method, it allows the grid spacing in the main-stream direction to be freely chosen.

A greater innovation is the choice of cross-stream variable; for this we adopt the *non-dimensional* stream function, ω, defined so that ω always equals zero at one edge of the boundary layer and unity at the other. The procedure combines the advantages of stream-line coordinates with those of restricting the boundary layer to a finite domain.

Real boundary layers seldom have observable "edges", so those which are used to normalize the stream function are artificial; but they may be freely chosen; and we have devised a method of choosing them, during the course of the integration procedure, which ensures computational efficiency.

Although the method is a general one for parabolic equations, it is here illustrated by reference to equations having particular physical significance, i.e. to those expressing the laws of conservation of momentum, material, and energy (of various kinds). These equations are assembled, and expressed in the appropriate coordinate system, in Section 2; there we also introduce certain auxiliary relations which are appropriate to turbulent flow; and the main features of the grid-control technique are described in sub-section 2.4. The procedure of numerical solution is described in Section 3; its use is illustrated in Section 4, by calculations of three phenomena: a laminar boundary layer, a free turbulent flow, and a turbulent wall jet.

2. THE EQUATIONS OF THE BOUNDARY LAYER

2.1. *The partial differential equations for axi-symmetrical flow*

The coordinate system. Figure 2 illustrates the coordinate system which will be adopted for the axi-symmetrical flow to which attention will be confined.† The coordinate directions 1 and 2 are orthogonal, or nearly so; the values of the coordinates are ξ_1 and ξ_2, so defined that the element of distance ds in a plane through the axis of symmetry is given by:

$$ds = \sqrt{[(l_1\, d\xi_1)^2 + (l_2\, d\xi_2)^2]}. \qquad (2.1.1)$$

The length scales l_1 and l_2 remain to be defined.

† Plane flows are, of course, members of the axi-symmetrical family.

The direction of the constant-ξ_2 lines is chosen so that, for the most part, it is nearly parallel to the local direction of the component of the velocity vector in the plane of the diagram.

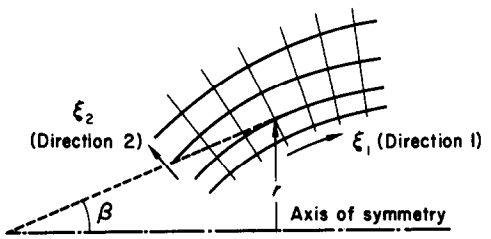

FIG. 2. Co-ordinate system for axi-symmetrical flow.

The constant-ξ_2 lines make the angle β with the symmetry axis; the angle is of course, in general, a function of ξ_1 and ξ_2. The constant-ξ_1 lines are, correspondingly, everywhere almost perpendicular to stream lines. It will be supposed, as part of the boundary-layer approximation, that the heat-conduction, diffusion and viscous-action vectors have significant components only in direction 2.

The equations. We start from the following forms of the differential equations expressing the main conservation laws of steady flow. The symbols employed are defined in the Nomenclature.

Mass conservation:

$$\frac{\partial}{\partial \xi_1}(rl_2G_1) + \frac{\partial}{\partial \xi_2}(rl_1G_2) = 0, \tag{2.1.2}$$

or, alternatively:

$$\rho V_1 = G_1 = \frac{1}{rl_2}\frac{\partial \psi}{\partial \xi_2},$$

$$\rho V_2 = G_2 = \frac{-1}{rl_1}\frac{\partial \psi}{\partial \xi_1}. \tag{2.1.3}$$

Momentum conservation in direction 1:

$$\frac{G_1}{l_1}\frac{\partial V_1}{\partial \xi_1} + \frac{G_2}{l_2}\frac{\partial V_1}{\partial \xi_2} = \frac{1}{rl_1l_2}\frac{\partial}{\partial \xi_2}\left(\frac{rl_1}{l_2}\mu_{1,\text{eff}}\frac{\partial V_1}{\partial \xi_2}\right) - \frac{1}{l_1}\frac{\partial p}{\partial \xi_1} + V_2G_1\frac{\partial \beta}{\partial \xi_1} + \frac{V_\theta G_\theta}{r}\sin\beta. \tag{2.1.4}$$

Momentum conservation in direction 2:

$$0 = \frac{-1}{l_2}\frac{\partial p}{\partial \xi_2} - \frac{V_1G_1}{l_1}\frac{\partial \beta}{\partial \xi_1} + \frac{V_\theta G_\theta}{r}\cos\beta. \tag{2.1.5}$$

Momentum conservation in direction θ:

$$\frac{G_1}{l_1}\frac{\partial V_\theta}{\partial \xi_1} + \frac{G_2}{l_2}\frac{\partial V_\theta}{\partial \xi_2} = \frac{1}{rl_1l_2}\frac{\partial}{\partial \xi_2} \times \left(r^2\frac{l_1}{l_2}\frac{\mu_{1,\text{eff}}}{\sigma_{\theta,\text{eff}}}\frac{\partial (V_\theta/r)}{\partial \xi_2}\right) - \frac{V_rG_\theta}{r}. \tag{2.1.6}$$

Equation for stagnation enthalpy, $\tilde{h}$:

$$\frac{G_1}{l_1}\frac{\partial \tilde{h}}{\partial \xi_1} + \frac{G_2}{l_2}\frac{\partial \tilde{h}}{\partial \xi_2} = \frac{1}{rl_1l_2}\frac{\partial}{\partial \xi_2}\left[\frac{rl_1}{l_2}\mu_{1,\text{eff}} \times \left\{\frac{1}{\sigma_{h,\text{eff}}}\frac{\partial \tilde{h}}{\partial \xi_2} + \left(\frac{1}{\sigma_{k,\text{eff}}} - \frac{1}{\sigma_{h,\text{eff}}}\right)\frac{\partial k}{\partial \xi_2} + \left(1 - \frac{1}{\sigma_{h,\text{eff}}}\right)\frac{\partial}{\partial \xi_2}\left(\frac{V_1^2}{2}\right) + \left(\frac{1}{\sigma_{\theta,\text{eff}}} - \frac{1}{\sigma_{h,\text{eff}}}\right)\frac{\partial}{\partial \xi_2}\left(\frac{V_\theta^2}{2}\right) - \frac{1}{\sigma_{\theta,\text{eff}}} \times \frac{l_2^2}{rl_1}V_\theta^2\cos\beta\right\}\right]. \tag{2.1.7}$$

Conservation of chemical species j:

$$\frac{G_1}{l_1}\frac{\partial m_j}{\partial \xi_1} + \frac{G_2}{l_2}\frac{\partial m_j}{\partial \xi_2} = \frac{1}{rl_1l_2}\frac{\partial}{\partial \xi_2}\left(\frac{rl_1}{l_2}\frac{\mu_{1,\text{eff}}}{\sigma_{j,\text{eff}}}\frac{\partial m_j}{\partial \xi_2}\right) + R_j. \tag{2.1.8}$$

Conservation of kinetic energy of turbulence, k:

$$\frac{G_1}{l_1}\frac{\partial k}{\partial \xi_1} + \frac{G_2}{l_2}\frac{\partial k}{\partial \xi_2} = \frac{1}{rl_1l_2}\frac{\partial}{\partial \xi_2} \times \left(\frac{rl_1}{l_2}\frac{\mu_{1,\text{eff}}}{\sigma_{k,\text{eff}}}\frac{\partial k}{\partial \xi_2}\right) + \mu_{1,\text{eff}}\left\{\left(\frac{1}{l_2}\frac{\partial V_1}{\partial \xi_2}\right)^2 + \frac{1}{\sigma_{\theta,\text{eff}}}\left[\frac{r}{l_2}\frac{\partial (V_\theta/r)}{\partial \xi_2}\right]^2\right\} - D_k. \tag{2.1.9}$$

All of these equations, except (2.1.2), (2.1.3) and (2.1.5), can be regarded as possessing the

common form:

$$\frac{G_1}{l_1}\frac{\partial\phi}{\partial\xi_1}+\frac{G_2}{l_2}\frac{\partial\phi}{\partial\xi_2}=\frac{1}{l_1 l_2 r}\frac{\partial}{\partial\xi_2}\times\left(\frac{rl_1}{l_2}\frac{\mu_{1,\text{eff}}}{\sigma_{\phi,\text{eff}}}\frac{\partial\phi}{\partial\xi_2}\right)+\Phi. \quad (2.1.10)$$

Here ϕ stands for any of the dependent variables: V_1, V_θ, $\tilde{h}$, m_j, k; and Φ stands for terms appearing on the right-hand side which do not contain $\partial\phi/\partial\xi_2$. Specifically, the meanings of Φ can be expressed by the following table.

Table 1. Significances of Φ

When ϕ stands for:	Φ stands for:
V_1	$\frac{-1}{l_1}\frac{\partial p}{\partial\xi_1}+V_2G_1\frac{\partial\beta}{\partial\xi_2}+\frac{V_\theta G_\theta}{r}\sin\beta$
V_θ	$\frac{-1}{rl_1l_2}\frac{\partial}{\partial\xi_2}\left(l_1\frac{\mu_{1,\text{eff}}}{\sigma_{\theta,\text{eff}}}V_\theta\cos\beta\right)-\frac{V_rG_\theta}{r}$
$\tilde{h}$	$\frac{1}{rl_1l_2}\frac{\partial}{\partial\xi_2}\left[\frac{rl_1}{l_2}\mu_{1,\text{eff}}\left\{\left(\frac{1}{\sigma_{k,\text{eff}}}-\frac{1}{\sigma_{h,\text{eff}}}\right)\frac{\partial k}{\partial\xi_2}+\left(1-\frac{1}{\sigma_{h,\text{eff}}}\right)\frac{\partial}{\partial\xi_2}\times\left(\frac{V_1^2}{2}\right)+\left(\frac{1}{\sigma_{\theta,\text{eff}}}-\frac{1}{\sigma_{h,\text{eff}}}\right)\times\frac{\partial}{\partial\xi_2}\left(\frac{V_\theta^2}{2}\right)-\frac{1}{\sigma_{\theta,\text{eff}}}\frac{l_2^2}{rl_1}V_\theta^2\cos\beta\right\}\right]$
m_j	R_j
k	$\mu_{1,\text{eff}}\left\{\left(\frac{1}{l_2}\frac{\partial V_1}{\partial\xi_2}\right)^2+\frac{1}{\sigma_{\theta,\text{eff}}}\left(\frac{r}{l_2}\frac{\partial(V_\theta/r)}{\partial\xi_2}\right)^2\right\}-D_k$

The similarity of their equations allows a common treatment for the variables V_1, V_θ, $\tilde{h}$, m_j and k. The equations expressing conservation of mass and of direction-2 momentum will be handled differently.

The transformation to ω as cross-stream variable. As yet l_1 and l_2 have not been defined. We now make a choice of l_2 which gives ξ_2 the significance of the non-dimensional stream function, for which we adopt the special symbol ω; thus

$$\xi_2=\omega\equiv\frac{\psi-\psi_I}{\psi_E-\psi_I}. \quad (2.1.11)$$

Here ψ_I and ψ_E are the values of ψ prevailing at the internal (I) and external† (E) boundaries of the region which is to be considered; they are functions of ξ_1 which may be selected arbitrarily, but which we shall try to choose so that all the important variations in the dependent variables take place at ψ values between ψ_I and ψ_E.

Equation (2.1.11) implies:

$$\frac{\partial\psi}{\partial\xi_1}=(1-\omega)\frac{d\psi_I}{d\xi_1}+\omega\frac{d\psi_E}{d\xi_1}, \quad (2.1.12)$$

and:

$$\frac{\partial\psi}{\partial\xi_2}=\frac{\partial\psi}{\partial\omega}=\psi_E-\psi_I. \quad (2.1.13)$$

These relations may be substituted into the two parts of equation (2.1.3), which expresses the mass-conservation principle. The first part gives the required relation for l_2, while the second gives an expression for G_2. Thus:

$$l_2=\frac{\psi_E-\psi_I}{rG_1}, \quad (2.1.14)$$

and:

$$G_2=\frac{-1}{rl_1}\left\{(1-\omega)\frac{d\psi_I}{d\xi_1}+\omega\frac{d\psi_E}{d\xi_1}\right\}. \quad (2.1.15)$$

Substitution of these two results into the general differential equation (2.1.10) yields the

† The labels "internal" and "external" are most apt for axi-symmetrical coordinate systems for which ξ_2 increases with distance in the radial direction. However, being only labels, they can be used generally also.

following new form of this equation:

$$\frac{\partial\phi}{\partial\xi_1} - \frac{1}{(\psi_E - \psi_I)}\left\{(1-\omega)\frac{d\psi_I}{d\xi_1} + \omega\frac{d\psi_E}{d\xi_1}\right\}\frac{\partial\phi}{\partial\omega} = \frac{1}{(\psi_E - \psi_I)^2}\frac{\partial}{\partial\omega}\left(\frac{r^2 l_1 G_1 \mu_{1,\text{eff}}}{\sigma_{\phi,\text{eff}}}\frac{\partial\phi}{\partial\omega}\right) + \Phi\frac{l_1}{G_1}. \quad (2.1.16)$$

It is this equation which forms the starting point for the finite-difference procedure.

The direction-2 momentum equation. Equation (2.1.5) can be integrated along a line of constant ξ_1 to give:

$$p - p_I = \int_{\xi_{2,I}}^{\xi_2}\left(-\frac{V_1 G_1}{l_1}\frac{l_2\,\partial\beta}{\partial\xi_1} + \frac{V_\theta G_\theta}{r} l_2\cos\beta\right)d\xi_2. \quad (2.1.17)$$

Substitution from equation (2.1.14), with ω written in place of ξ_2, yields:

$$p - p_I = (\psi_E - \psi_I)\int_0^\omega\left(\frac{-V_1\,\partial\beta}{l_1 r\,\partial\xi_1} + \frac{V_\theta G_\theta}{r^2 G_1}\cos\beta\right)d\omega. \quad (2.1.18)$$

This equation must also be used, in general, during the finite-difference solution procedure. When, however, $\partial\beta/\partial\xi_1$ is negligible, as is often the case, and when the rotational velocity V_θ is negligible, equation (2.1.18) reduces simply to: $p = p_I = p_E$; the pressure can be taken as uniform across the boundary layer.

2.2. *Auxiliary relations*

Geometrical relations. Appearing in equations (2.1.16) and (2.1.18) are the geometrical quantities: r, l_1 and β. It is necessary to calculate these as functions of the independent variables ξ_1 and ω. An example will suffice to show how these calculations can be made.

Suppose that the boundary-layer region is bounded by a solid surface of rotation, as shown in Fig. 3. Then the direction 1 can be taken as parallel to this surface and the direction 2 (ω-direction) as normal to it. Now suppose that, along the surface, where ω equals zero, l_1 equals unity; then ξ_1 stands for the distance along the surface.

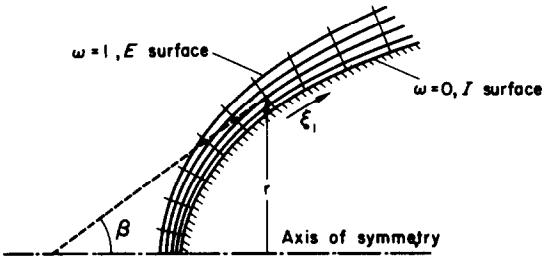

FIG. 3. Illustration of a typical coordinate system.

If constant-ξ_1 lines are normals to the surface, and if the coordinate system can be treated as orthogonal, β is a function of ξ_1 alone; moreover the function is prescribed by the shape of the surface, which we may suppose to be known. A consequence is that the length-scale factor l_1 is given by:

$$\xi_1 = \text{fixed}: l_1 = 1 - \left(\frac{\partial\beta}{\partial\xi_1}\right)\int_0^\omega l_2\,d\omega, \quad (2.2.1)$$

where l_2, of course, varies with ω in accordance with equation (2.1.14) and the velocity distribution.

The radius r is also calculable from simple geometrical considerations. The relevant formula is:

$$\xi_1 = \text{fixed}: \quad r = r_I + (\cos\beta)\int_0^\omega l_2\,d\omega. \quad (2.2.2)$$

The quantity $\int_0^\omega l_2\,d\omega$, it should be understood, equals the distance from the wall measured along a line of constant ξ_1.

In the case illustrated in Fig. 2, the decision to locate the I-surface along the wall requires no justification; but it should be recognized that it is a free decision, not a forced one. Where to place the E-surface is not at first obvious; we

can repeat only that we want the region between the two surfaces to contain all the points at which viscous, diffusion and heat-conduction effects are significant. How this can be ensured will be described in Section 2.4 below.

Exchange coefficients. Equations are needed which will connect $\mu_{1,\text{eff}}$, and the exchange-coefficient ratios $\sigma_{\theta,\text{eff}}$, $\sigma_{h,\text{eff}}$, $\sigma_{k,\text{eff}}$ and $\sigma_{j,\text{eff}}$, with the dependent variables of the calculation.

If the flow is laminar, $\mu_{1,\text{eff}}$ is the laminar viscosity; standard data sources allow this to be connected quantitatively with the enthalpy and composition of the fluid. Then also $\sigma_{\theta,\text{eff}}$ equals unity, because the laminar viscosity is isotropic; and $\sigma_{k,\text{eff}}$ becomes unimportant because k is zero. The quantities $\sigma_{h,\text{eff}}$ and $\sigma_{j,\text{eff}}$ are respectively the Prandtl number and the Schmidt number, on which standard data sources once again give information.†

When the flow is turbulent, different relationships are appropriate. Usually each σ_{eff} is taken as uniform in the turbulent region, and approximately equal to unity; the main interest centres on the calculation of $\mu_{1,\text{eff}}$.

One formula in common use is that of Prandtl [5]. This may be written as:

$$\mu_{1,\text{eff}} = \frac{l_m^2 \rho}{l_2} \left| \frac{\partial V_1}{\partial \xi_2} \right| \tag{2.2.3}$$

where l_m is the so-called mixing length. The latter quantity is usually taken as dependent on the distance from the wall; $\int_0^\omega l_2 \, d\omega$; examples are given below (Section 4).

Another formula, proposed by Kolmogorov [6] and Prandtl [7] connects the viscosity with the kinetic energy of turbulence, and another length scale, l_k. This has been used by Monin [8] and Glushko [9], among others. The formula may be expressed as:

$$\mu_{1,\text{eff}} = l_k \rho k^{\frac{1}{2}}. \tag{2.2.4}$$

The length scale l_k is also taken as some function of distance from the wall.

Particularly when V_θ is of the same order of magnitude as V_1, more elaborate formulae for $\mu_{1,\text{eff}}$ are needed to express experimental findings. All known proposals could be easily incorporated into the solution procedure that is to be described; there is therefore no necessity to introduce further examples.

The dissipation-rate. Since the employment of equation (2.2.4) necessitates solution of the differential equation for the kinetic energy of turbulence, equation (2.1.9), it is appropriate to mention that the dissipation-rate D_k must enter an auxiliary relation. An example, in accordance with dimensional analysis, is;

$$D_k = \text{constant} \, . \, \rho k^{\frac{3}{2}} / l_k. \tag{2.2.5}$$

Here l_k is of course the same as the quantity appearing in equation (2.2.4).

Equations (2.2.4) and (2.2.5) are recommended, it should be added, only where the flow is fully turbulent. This condition can be expressed in terms of a "local Reynolds number of turbulence": $l_k \rho k^{\frac{1}{2}}/\mu$ should be very much greater than unity. What functions are appropriate when the condition is not fulfilled is not at present clear.

Thermodynamic relationships. The dependent variables are linked by many relations which express either, definitions, or thermodynamic laws, or material-property relationships. Among these is:

$$\tilde{h} \equiv h + \frac{V_1^2}{2} + \frac{V_\theta^2}{2} + k, \tag{2.2.6}$$

where h is the specific enthalpy; the kinetic energy associated with direction-2 motion is neglected. Equation (2.2.6) allows the enthalpy to be calculated from the values of $\tilde{h}$, V_1, V_θ and k appearing in the solutions of the differential equations. If the equation for k is not being solved for use in a viscosity relation like (2.2.4),

† Strictly speaking, in laminar flow, $\sigma_{h,\text{eff}}$ reduces to the Prandtl number only under certain conditions (e.g. equal specific heats for all components, and no chemical reaction; or, uniform composition). There is, however, no point in discussing the exceptions here.

it is usual to drop this equation and neglect the contributions of k to $\tilde{h}$.

Other important properties linked to enthalpy and concentration by thermodynamic relations are the temperature T, and the density ρ. The equations are too well known to require presentation.

2.3. *Initial and boundary conditions*

The domain of integration. The solutions of the equations are to be confined to the region: $\xi_1 \geqslant \xi_{1,0}$, $0 \leqslant \omega \leqslant 1$. Figure 4 illustrates this. There is no need to specify the right-hand edge of the domain.

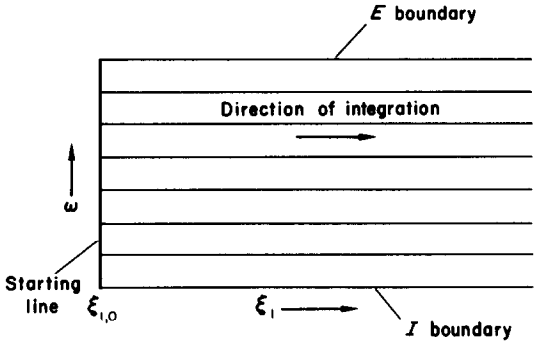

FIG. 4. The domain of integration.

In order to integrate the parabolic equations, it is necessary to know values of all the variables along the "starting line" where ξ_1 equals $\xi_{1,0}$; these values comprise the initial conditions. We shall suppose that they are always available.

Equally necessary is information about conditions at the I and E boundaries. This information may be in the form of prescribed distributions of the values of the variables along these lines; alternatively, values of gradients, or other functions, of the variables may be prescribed. Some special kinds of boundary condition will be mentioned in the present section.

The pressure should be prescribed along a single boundary; for only one integration constant is required for equation (2.1.18). Two types of prescription will be mentioned below.

Wall-flux laws for turbulent flow. When the boundary layer is turbulent and a solid wall is present, the region near the wall exhibits very steep gradients of velocity, and often of other variables too. Since the velocity is also low there, the $\partial\phi/\partial\xi_1$ term is locally negligible in the differential equation;† consequently the variation of ϕ can be calculated by reference to the remaining terms, which involve differential coefficients with respect to ω alone. Thus a "Couette-flow analysis" gives a good approximation to the exact solution of the equation.

It is possible, but somewhat wasteful, to crowd together the constant-ω grid lines in the region near a wall so as to perform this Couette-flow analysis at each step of the finite-difference solution procedure. But it is also possible, and more economical, to carry out Couette-flow analyses, once for all, before the particular finite-difference calculation is started; the results of these analyses can then be incorporated into algebraic relationships which serve as boundary conditions. The economy arises from the resulting freedom to have the constant-ω lines more evenly spaced; it suffices, for example, to have one which lies somewhat beyond the outer edge of the "laminar sub-layer", and to connect values of variables and fluxes there, to values and fluxes at the wall, by way of algebraic formulae. A simple example of such a formula is presented in Section 4.3 below. More elaborate formulae will be found in [10]. They have the general form:

$$\frac{\left(\dfrac{\mu}{\sigma_\phi l_2}\dfrac{\partial\phi}{\partial\omega}\right)_S}{(\phi_{S+}-\phi_S)\,G_{1,S+}} = S_{\phi,S}\left(\frac{G_{1,S+}\displaystyle\int_0^{\omega_{S+}} l_2\,\mathrm{d}\omega}{\mu_S}, \sigma_{\phi,S}, \ldots\right). \qquad (2.3.1)$$

† This fact is best understood by reference to equation (2.1.4), with l_1 and l_2 put equal to unity; it is disguised in equation (2.1.16) by the fact that the definition of ω contains G_1. The fact is well known to laminar- boundary-layer specialists, and easily proved.

Here the subscript S denotes the solid-surface boundary, either E or I, and $S+$ denotes the nearest grid point to S; μ is the laminar viscosity of the fluid; and σ_ϕ is the laminar Prandtl or Schmidt number appropriate to property ϕ. The numerator of the left-hand side has the significance of the flux of ϕ across the boundary; the function $S_{\phi,S}$ is a Stanton number, having as its main argument the Reynolds number

$$(G_{1,S+} \int_0^{\omega_{S+}} l_2 \, \mathrm{d}\omega/\mu_S)$$

and the laminar Prandtl or Schmidt number. Other arguments may account for the presence of mass transfer, roughness, pressure gradient and property variations; but they involve quantities appropriate to points S and $S+$ alone.

When the flux through the wall is given, equation (2.3.1) is used for the calculation of ϕ_S; when, on the other hand, ϕ_S is given, the flux through the wall is calculated. These remarks apply whether ϕ stands for temperature, enthalpy, concentration, velocity, or any other entity for which equation (2.1.10) is valid; of course, different words are used to describe the various cases; for example, the "Stanton number of momentum transfer" is better known as "one half of the drag coefficient".

Other conditions at the boundaries. When the I or E boundary does not coincide with a wall, it is usual for the values of the dependent variables to be prescribed there; for example, if the variable is k, the kinetic energy of the fluctuating motion, its value on the boundary will ordinarily be that which prevails in the stream to which the domain of integration is adjacent.

If the boundary coincides with the symmetry axis, the gradient of ϕ with respect to normal distance must be zero. This fact can serve as a boundary condition in appropriate circumstances, for example when the centre-line of an axi-symmetrical jet is in question.

The prescription of the pressure. It has already been mentioned that an equation exists, namely (2.1.18), from which the pressure at any point along the constant-ξ_1 line can be calculated whenever *one* pressure is prescribed; this could be either p_I or p_E. Often this prescription is given through the velocity at a boundary, coupled with the statement that pressure, velocity and density are linked there by the Euler equation, i.e. by equation (2.1.4), with the shear-stress term neglected. This situation usually arises in external-flow situations, for example boundary layers on aerofoils, and free jets.

When the flow is an internal one, like that in a diffuser for example, neither pressure nor velocity can be calculated directly from input data. Instead, the continuity equation must be solved for the whole flow; this gives an additional condition to be satisfied by the velocity and density profiles at the next step of the integration; it must be solved simultaneously with equations which represent the finite-difference form of the differential equation. Further discussion will be deferred until these equations have been introduced, in Section 3.3 below.

2.4. *The choice of ψ_I and ψ_E*

The purpose. ψ_I and ψ_E, it will be remembered, are functions of ξ_1 which we are still free to specify as we wish. The requirements are: that the constant-ξ_1 lines will be approximately normal to stream lines, at any rate in the regions of highest velocity; and that the region $0 \leqslant \omega \leqslant 1$ contains all points having significant ϕ gradients.

Because, in boundary layers, gradients are finite only in *slender* regions, for which the long dimension is roughly parallel to the flow direction, fulfilment of the second requirement satisfies the first one also. We shall now describe some suitable procedures for controlling ψ_I and ψ_E.

The symmetry axis as a boundary. If the region in which gradients are significant encloses the symmetry axis, as in the case of a wake behind a cylinder in longitudinal flow,

the choice for ψ_I is obvious; it should be placed equal to a constant, for example zero.

A solid wall as a boundary. When the region containing significant gradients extends right up to a solid wall, as in the case of the flow in a diffuser, the objective can be achieved by making one of the boundaries coincide with the wall. Let us use the subscript S once more to denote this boundary. If the wall is impermeable, ψ_S must be a constant, which can be arbitrarily fixed; if it is permeable, however, ψ_S must vary in accordance with equation (2.1.15), which reduces (for ω equal to zero or unity as appropriate) to:

$$G_{2,S} = \frac{-1}{rl_1}\frac{\mathrm{d}\psi_S}{\mathrm{d}\xi_1}. \tag{2.4.1}$$

In some cases, $G_{2,S}$, the mass-transfer rate across the wall, is fixed by the data of the problem; this occurs, for example, when suction of the boundary layer through the wall is effected by external means. In other cases, as when sublimation occurs from the solid into the gas at a rate controlled by heat transfer, $G_{2,S}$ has to be calculated at each stage from the local values of some of the ϕ's. Always, however, a differential equation is obtained for ψ_S; this can be solved, by the usual numerical techniques, during the course of the integration.

When the boundary is free. The last two choices for boundary-ψ values were so straightforward that they merited discussion only to serve as contrasts to that which now confronts us: the choice of the value of the stream function along the boundary separating the region of interest from an adjoining region of the flow in which the gradients are negligible. This boundary might be the outer "edge" of an axi-symmetrical turbulent jet, injected into a moving stream; the outer "edge" of the laminar boundary layer on a flat plate is another example. We shall use the subscript G to denote such a boundary.

Two cases of this kind must now be distinguished. In the first, a definite edge to the boundary layer can be established without arbitrariness; this case arises when the flow is turbulent and may be assumed to obey the Prandtl 1925 mixing-length hypothesis [5]; for then, as may be seen from [11] for example, the transport properties all vanish along a surface which is not infinitely remote from the region. Of course, this vanishing applies only when the laminar contribution to the transport properties is already being neglected. Since this neglect is justified only where the turbulent component is *large*, the case may be regarded as rather artificial; nevertheless, it is simple, useful, and sufficiently accurate for most purposes.

In the second case of a free boundary, the transport properties neither vanish, nor fall to a small fraction of their values elsewhere, along a definite boundary line. This is true of laminar flows, and of turbulent ones which are supposed to obey the Kolmogorov–Prandtl [6, 7] postulate, for example, and for which the free-stream turbulence level may not be neglected. In this case the G boundary is more arbitrary.

Free-stream boundary with vanishing transport properties. When $\mu_{1,\mathrm{eff}}$ (say) vanishes along the G boundary, a differential equation for ψ_G can be obtained from the general partial differential equation (2.1.16). Just outside the G boundary, $\partial\phi/\partial\omega$ is zero; the equation therefore reduces to:

$$\left(\frac{\partial\phi}{\partial\xi_1}\right)_G = \left(\Phi\frac{l_1}{G_1}\right)_G \tag{2.4.2}$$

Consideration of a point just inside the G boundary, for which $\partial\phi/\partial\xi_1$ and $(\Phi l_1/G_1)$ cannot be significantly different, therefore leads (whether ω equals zero or unity at the boundary designated by subscript G) to:

$$-\frac{\mathrm{d}\psi_G}{\mathrm{d}\xi_1} = \frac{1}{(\psi_E - \psi_I)} \lim_{\omega\to\omega_G}\left[\frac{\dfrac{\partial}{\partial\omega}\left(\dfrac{r^2 l_1 G_1 \mu_{1,\mathrm{eff}}\cdot\partial\phi}{\sigma_{\phi,\mathrm{eff}}\quad\partial\omega}\right)}{\dfrac{\partial\phi}{\partial\omega}}\right]. \tag{2.4.3}$$

Here we see, incidentally, an implied test discriminating between the two cases. If $\mu_{1,\text{eff}}$ is proportional to $\partial\phi/\partial\omega$, the limit will be finite (because $r^2 l_1 G_1/\sigma_{\phi,\text{eff}}$ is finite); then a real boundary can indeed exist. Otherwise the limit does not converge; $d\psi_G/d\xi_1$ becomes infinite; ψ_G must be infinite; so *all* the fluid must be contained within the range $0 \leqslant \omega \leqslant 1$.

When the limit converges, which is true when Prandtl's 1925 mixing-length hypothesis is used, equation (2.4.3) provides a satisfactory specification of $d\psi_G/d\xi_1$. With its aid, the ψ_G values along the boundaries can be calculated during the course of integration, just as in the case of ψ_S. These calculations of the boundary values of ψ achieve the desired effect of causing the coordinate grid to expand and contract so as always to meet the requirement for computational efficiency.

Free-stream boundary with non-vanishing transport properties. Since the limit in equation (2.4.3) does not converge unless the transport property vanishes, we shall apply now the full partial differential equation (2.1.16) just inside the G boundary with a special consideration for evaluating the $\partial\phi(\partial\xi_1$ term: we shall seek to locate the boundary so that, on the grid line just inside the G boundary, the value of ϕ will be equal to a predetermined number ϕ^*. This number can be chosen, for example, so that the difference $(\phi_G - \phi^*)$ is a certain small percentage of the maximum ϕ-difference across the layer. Now the value of $\partial\phi/\partial\xi_1$ can be calculated along the grid line just inside the G boundary from the current known value of ϕ and the value of ϕ^* desired at the downstream station. The finite-difference formula for this will be given in Section 3.6 below. It is sufficient to note here that, if the value of ϕ^* is properly chosen, we can be sure that the grid will always conform to the region in which significant gradients of ϕ are present.

The above procedures have been outlined as ones which seem best at present. However, it should be remembered that the "entrainment rate" $d\psi_G/d\xi_1$ is in any case arbitrary; its sole justification is computational efficiency. It is, therefore, permissible to abandon the above procedures at any time that it becomes convenient to do so; for example, one may put a maximum limit on the entrainment rate to avoid excessive curvature of the streamlines near the boundary.

2.5. *Closure to section*

Now that formulae have been indicated with the aid of which the boundary-ψ's can be calculated, the whole mathematical structure has been outlined. It remains to show how the equations can be solved; this is the function of the following sections. The finite-difference procedures are explained in Section 3, while Section 4 demonstrates their utility by way of examples.

3. THE RECOMMENDED FINITE-DIFFERENCE PROCEDURE

3.1. *Outline*

For convenience, let us express equation (2.1.16) as:

$$\frac{\partial\phi}{\partial\xi_1} + (a + b\omega)\frac{\partial\phi}{\partial\omega} = \frac{\partial}{\partial\omega}\left(c\frac{\partial\phi}{\partial\omega}\right) + \Phi\frac{l_1}{G_1}, \tag{3.1.1}$$

where

$$a \equiv -\frac{1}{(\psi_E - \psi_I)}\frac{d\psi_I}{d\xi_1}, \tag{3.1.2}$$

$$b \equiv -\frac{1}{(\psi_E - \psi_I)}\frac{d(\psi_E - \psi_I)}{d\xi_1}, \tag{3.1.3}$$

and

$$c \equiv \frac{G_1 r^2 l_1 \mu_{1,\text{eff}}}{(\psi_E - \psi_I)^2 \sigma_{\phi,\text{eff}}}. \tag{3.1.4}$$

We shall solve equations of this type by step-by-step forward integration. Therefore, at every step in the integration, the values of ϕ will be known at discrete values of ω and at one value of ξ_1; our task will be to obtain the values of

ϕ at the same values of ω, but at a downstream value of ξ_1. By repetition of this basic operation, the whole field of interest can be covered.

The discrete values of ω and ξ_1, which are decided beforehand, define a grid; a portion of this is shown in Fig. 5. Points U and D represent respectively the upstream and downstream points at a given ω; points at nearby values of ω will be called $U+$, $U-$, $D+$, $D-$. The

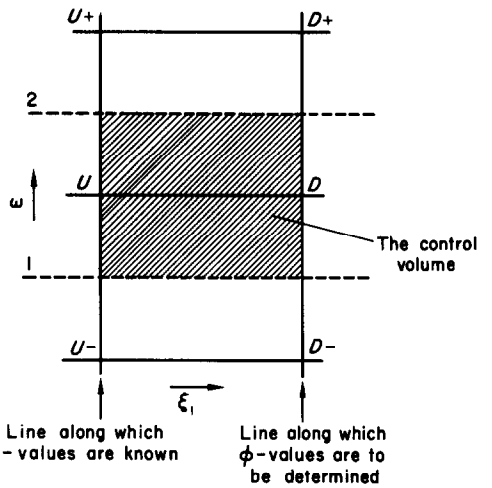

FIG. 5. Location of points referred to in the difference equation.

dashed lines 1 and 2 are the lines of constant ω, midway between $UU-$ and $UU+$ respectively. Lines 1 and 2 form, together with the two lines of constant ξ_1, a control volume (shown shaded) which will be useful for expressing the convection terms.

We shall describe in Section 3.2 below how equation (3.1.1) can be put in finite-difference form. Our representation of the convection terms, i.e. the terms on the left-hand side of equation (3.1.1), is based on an integrated average over a small control volume. This implies that the convection to point D is influenced by the values of ϕ at all the neighbouring points; it thus increases stability. Also, the integral equation over the whole layer is then automatically satisfied. While expressing the second-order term $\partial/\partial\omega(c\,\partial\phi/\partial\omega)$, we need to decide the value of ξ_1 at which this term will be evaluated. In general, we can use:

$$f\left[\frac{\partial}{\partial\omega}\left(c\frac{\partial\phi}{\partial\omega}\right)\right]_U + (1-f)\left[\frac{\partial}{\partial\omega}\left(c\frac{\partial\phi}{\partial\omega}\right)\right]_D,$$

where f is a number between zero and unity and subscripts U and D denote locations of evaluation. When f is unity, this form reduces to that of the explicit method, which, as mentioned earlier, has severe limitations on the step-length $(\xi_{1,D} - \xi_{1,U})$. For any value of f different from unity, the scheme becomes implicit. It can be shown, at least in simple cases, that instability is avoided if $0 \leqslant f \leqslant 0{\cdot}5$. The case of $f = 0{\cdot}5$ corresponds to the method of Crank and Nicholson [3]. We have decided to take the value of f as zero, as this combines stability with convenience. In other words, we shall evaluate the second-order term along the line $\xi_1 = \xi_{1,D}$.

3.2. *The difference formulae*

We shall now express the various terms in equation (3.1.1) by finite-difference formulae.

The convective terms. The terms on the left-hand side of equation (3.1.1) can be expressed as:

$$\frac{\int_{\xi_{1,U}}^{\xi_{1,D}}\int_{\omega_1}^{\omega_2}\left\{\frac{\partial\phi}{\partial\xi_1} + (a+b\omega)\frac{\partial\phi}{\partial\omega}\right\}\mathrm{d}\omega\,\mathrm{d}\xi_1}{(\omega_2-\omega_1)(\xi_{1,D}-\xi_{1,U})}.$$

Now if we assume that ϕ varies linearly between the grid points in both ξ_1 and ω directions, it is easy to express the above double integral in terms of the values of ϕ at U, $U+$, $U-$, D, $D+$ and $D-$. The resulting expression can be written as:

$$g_1\phi_{D+} + g_2\phi_D + g_3\phi_{D-} + g_4,$$

where the g's are obtainable in terms of known quantities, including the values of ϕ at $\xi_1 = \xi_{1,U}$. The detailed expressions for the g's will not be given here; they can be easily obtained by straightforward algebra.

The flux term. As mentioned in Section 3.1, the

second-order term $\partial/\partial\omega(c\,\partial\phi/\partial\omega)$, representing the diffusional flux, will be evaluated along the line $\xi_1 = \xi_{1,D}$. However, in order that the resulting difference equations become linear, we shall evaluate the *coefficient* c along $\xi_1 = \xi_{1,U}$ where all the quantities are known. Thus the finite-difference form of $\partial/\partial\omega(c\,\partial\phi/\partial\omega)$ will be:

$$\frac{2}{\omega_{D+} - \omega_{D-}}\left\{\frac{(c_{U+} + c_U)}{2}\frac{(\phi_{D+} - \phi_D)}{(\omega_{D+} - \omega_D)} - \frac{(c_U + c_{U-})}{2}\frac{(\phi_D - \phi_{D-})}{(\omega_D - \omega_{D-})}\right\}.$$

The alternative practice would be to evaluate the c's along $\xi_1 = \xi_{1,D}$; but then the solution of the resulting non-linear equations would need iteration. We shall not consider this possibility here.

The source term. Finally, we need to express the term $\Phi\, l_1/G_1$ in finite-difference form. The simplest procedure would be to evaluate this term from the known quantities at $\xi_{1,U}$. A better practice† is to express the term $\Phi\, l_1/G_1$ as:

$$(\Phi\, l_1/G_1)_U + \left[\frac{\partial}{\partial\phi}(\Phi\, l_1/G_1)\right]_U (\phi_D - \phi_U).$$

When ϕ stands for V_1, the pressure-gradient term $\partial p/\partial\xi_1$ appears in the corresponding expression for Φ. Since the pressure p will not always be known, this case needs special consideration. It is easy to see that the finite-difference form of $\partial p/\partial\xi_1$ will be:

$$\frac{p_D - p_U}{\xi_{1,D} - \xi_{1,U}}.$$

An addition relationship can be obtained for the unknown pressure p_D from equation (2.1.18). We can write:

$$p_D - p_{D-} = (\psi_E - \psi_I)\int_{\omega_{D-}}^{\omega_D}\left(-\frac{V_1}{l_1 r}\frac{\partial\beta}{\partial\xi_1} + \frac{V_\theta G_\theta}{r^2 G_1}\cos\beta\right)\mathrm{d}\omega. \qquad (3.2.1)$$

Although in principle it is possible to handle this complete equation, the increased algebraic complication may obscure the main elements of the procedure. Therefore, for the purposes of presentation only, we shall use a simpler form of equation (3.2.1): we shall assume that pressure p is uniform for a given value of ξ_1. This assumption is valid when the stream lines are not highly curved and the swirl velocity V_θ is small. Incidentally, this case happens to be the one of most practical importance. The following treatment is valid for this case. A reader interested in cases of non-uniform pressure in the ξ_2 direction can work out the full implications of equation (3.2.1) along similar lines.

The complete difference equation. So far, we have explained how the individual terms can be expressed in finite-difference form. Putting them together, we compile the complete difference equation as follows:

$$g_1\phi_{D+} + g_2\phi_D + g_3\phi_{D-} + g_4 = \frac{2}{\omega_{D+} - \omega_{D-}}\left\{\frac{(c_{U+} + c_U)}{2}\frac{(\phi_{D+} - \phi_D)}{(\omega_{D+} - \omega_D)} - \frac{(c_U + c_{U-})}{2}\frac{(\phi_D - \phi_{D-})}{(\omega_D - \omega_{D-})}\right\} + \left[\frac{\Phi\, l_1}{G_1}\right]_U + \left[\frac{\partial}{\partial\phi}(\Phi\, l_1/G_1)\right]_U (\phi_D - \phi_U). \qquad (3.2.2)$$

It is easy to see that, by rearrangement, this equation can be reduced to the form:

$$\phi_D = A\phi_{D+} + B\phi_{D-} + C, \qquad (3.2.3)$$

where A, B and C are obtainable in terms of known quantities. If the pressure p_D is given, then the equation for V_1 will also have the same form as (3.2.3); however, in the case of confined

† A still better one, it might appear, would be to employ a more elaborate expression which allows for the dependence of a single Φ on several different dependent variables. However, to do so would be to introduce more unknowns than can be coped with by the solution procedure which is advocated below; we therefore refrain from this elaboration.

flow, the pressure p_D will appear as unknown. The form of the equation will then be:

$$V_{1,D} = AV_{1,D+} + BV_{1,D-} + C + Dp_D. \quad (3.2.4)$$

Equation (3.2.3) or (3.2.4) is the final outcome of our finite-difference formulation. There will be one such equation for every grid point except for those on the I and E boundaries. Only in certain circumstances will the above-mentioned procedure need modification. We shall describe this point in Section 3.4 below. Now we turn to the problem of solving the algebraic equations like (3.2.3).

3.3. *Solution of the difference equations*

Procedure for unconfined flows. For unconfined flows, the pressure p_D can be obtained before solving the boundary-layer equations. Then the difference equations for all the ϕ's including V_1 are of the form (3.2.3).

Let us suppose that the grid lines divide the thickness of the layer into N strips. If subscript i denotes a node corresponding to a value of ω, then equations of the type (3.2.3) can be written as:

$$\phi_i = A_i\phi_{i+1} + B_i\phi_{i-1} + C_i, \quad (3.3.1)$$

for $i = 2, 3, 4, \ldots N$. The values of ϕ_1 and ϕ_{N+1} will be given as boundary conditions. (When the gradients of ϕ at the boundaries are given, we shall modify the formulation of equation (3.2.3) so that the following solution procedure can still be used. This point will be described in Section 3.4 below.) We shall first transform equation (3.3.1) into the following form:

$$\phi_i = P_i\phi_{i+1} + Q_i, \quad (3.3.2)$$

where

$$\left.\begin{aligned} P_i &= \frac{A_i}{1 - B_iP_{i-1}}, \\ Q_i &= \frac{B_iQ_{i-1} + C_i}{1 - B_iP_{i-1}}, \\ P_2 &= A_2 \end{aligned}\right\} \quad (3.3.3)$$

and

$$Q_2 = B_2\phi_1 + C_2.$$

After the calculation of P's and Q's, it is a simple matter to obtain ϕ's from equation (3.3.2) by successive substitution starting from ϕ_{N+1}.

Procedure for confined flows. When the flow is confined, the pressure p_D is not directly specified. On the other hand, we have an additional relationship that the rate of change of the total mass flow in the whole duct with the streamwise co-ordinate ξ_1 depends only on the mass-transfer rates at the confining walls. Since pressure p_D appears only in an equation for V_1, the equations for other ϕ's can be solved by the above procedure for unconfined flows. We therefore describe below the procedure for solving the equation for V_1, for confined flows. This is being presented here for the sake of completeness; however, it should be mentioned that we have not yet used this procedure for solving any actual problem and that the examples in Section 4 below are all of the unconfined-flow variety.

As shown in Section 3.2, the equation for V_1 has the form given by (3.2.4); we shall rewrite that equation as follows:

$$V_{1,i} = A_iV_{1,i+1} + B_iV_{1,i-1} + C_i + D_ip, \quad (3.3.4)$$

for

$$i = 2, 3, 4, \ldots N,$$

where p stands for the pressure along the line $\xi_1 = \xi_{1,D}$. This equation can be transformed into:

$$V_{1,i} = P_iV_{1,i+1} + Q_i + R_ip, \quad (3.3.5)$$

where

$$\left.\begin{aligned} P_i &= \frac{A_i}{1 - B_iP_{i-1}}, \\ Q_i &= \frac{B_iQ_{i-1} + C_i}{1 - B_iP_{i-1}}, \\ R_i &= \frac{B_iR_{i-1} + D_i}{1 - B_iP_{i-1}}; \\ P_2 &= A_2, \\ Q_2 &= B_2V_{1,1} + C_2, \\ R_2 &= D_2. \end{aligned}\right\} \quad (3.3.6)$$

We transform equation (3.3.5) once again to express all V_1's in terms of $V_{1,N+1}$, as follows:

$$V_{1,i} = E_i V_{1,N+1} + F_i + H_i p, \qquad (3.3.7)$$

where

$$\left.\begin{aligned} E_i &= P_i E_{i+1}, \\ F_i &= P_i F_{i+1} + Q_i, \\ H_i &= P_i H_{i+1} + R_i; \\ E_N &= P_N, \\ F_N &= Q_N, \\ H_N &= R_N; \\ E_{N+1} &= 1, \\ F_{N+1} &= H_{N+1} = 0. \end{aligned}\right\} \qquad (3.3.8)$$

$$\left[\int_0^1 \frac{d\omega}{G_1}\right]_D - \left[\int_0^1 \frac{d\omega}{G_1}\right]_U \approx \sum_{i=1}^{N} \frac{(\omega_{i+1} - \omega_i)}{0{\cdot}5(\rho_{i+1} + \rho_i)_U} \left\{\frac{-2}{(V_{1,i+1} + V_{1,i})^2}\right\}_U \times \{(V_{1,i+1} + V_{1,i})_D - (V_{1,i+1} + V_{1,i})_U\}, \qquad (3.3.10)$$

which has the form:

$$\sum_{i=2}^{N} L_i (V_{1,i+1} + V_{1,i})_D = M, \qquad (3.3.11)$$

where L's and M are known quantities. Now substituting from equation (3.3.7), we get, after some re-arrangement:

$$p = \frac{M - \sum_{i=2}^{N} L_i (E_{i+1} + E_i) V_{1,N+1} - \sum_{i=2}^{N} L_i (F_{i+1} + F_i)}{\sum_{i=2}^{N} L_i (H_{i+1} + H_i)}. \qquad (3.3.12)$$

At this stage we shall introduce the continuity equation for the whole duct. From equation (2.1.14) we see that:

$$\int_0^1 \frac{d\omega}{G_1} = \int_0^1 \frac{r l_2 \, d\omega}{(\psi_E - \psi_I)}. \qquad (3.3.9)$$

It is easy to see that the right-hand side is calculable for any value of ξ_1; because the variation of $(\psi_E - \psi_I)$ can be obtained from the prescribed mass-transfer rates at the confining walls, and the integral

$$\int_0^1 r l_2 \, d\omega$$

is known from the geometry of the duct. We can write†:

Using this value of p, we can obtain the values of all V_1's from equation (3.3.7).

3.4. *Special procedures*

It has been implicitly assumed so far that the values ϕ_1 and ϕ_{N+1} at the boundaries are known. Sometimes, however, instead of the value of ϕ, the gradient of ϕ is specified along the boundary. In such cases, the difference equations for the nodes near the boundary need some modification.

The equation (3.1.1) can be written as:

$$\frac{\partial \phi}{\partial \xi_1} + (a + b\omega)\frac{\partial \phi}{\partial \omega} = \frac{\partial}{\partial \omega}(r J_\phi) + \Phi \frac{l_1}{G_1}, \qquad (3.4.1)$$

where J_ϕ stands for the flux caused by the gradient of ϕ. Now, if the point $D-$ lies on the boundary, we can write the flux term $\partial/\partial\omega\,(rJ_\phi)$ in finite-difference form as follows:

$$\frac{2}{\omega_{D+} - \omega_{D-}} \left\{ \frac{(c_{U+} + c_U)}{2} \frac{(\phi_{D+} - \phi_D)}{(\omega_{D+} - \omega_D)} - \frac{(r_U + r_{U-})}{2} \cdot J_{\phi, D-} \right\},$$

† Here we neglect the density variations, so as to have only $V_{1,D}$'s as unknowns. A different practice will have to be adopted when the density variations have a significant effect on the pressure variations. For example, $\partial\rho/\partial\xi_1$ values can be stored in previous steps of the integration, and used for forward extrapolation here. It is however premature to suggest remedies for difficulties that have not yet been encountered.

where $J_{\phi,D-}$ is known from the prescribed gradient of ϕ at the boundary. This formulation avoids explicit reference to the unknown boundary value ϕ_{D-}. Of course, when all other ϕ's have been calculated, ϕ_{D-} can be deduced from the prescribed gradient and from the value of ϕ_D.

3.5. *Choice of forward step*

To perform the forward integration, the size of the step length $(\xi_{1,D} - \xi_{1,U})$ must be decided. Since the present finite-difference formulation is of implicit type, stability will be maintained even when the size of the step is large; however, for good accuracy, small steps are necessary. The most economical size of the step for a particular class of problem can be found by experience. A simple procedure is to make the step length proportional to the thickness of the layer, i.e. to put:

$$(\xi_{1,D} - \xi_{1,U}) = \text{const.} \times \frac{1}{l_1}\int_0^1 l_2 \, d\omega. \qquad (3.5.1)$$

This will be quite satisfactory for most of the turbulent boundary layers where the thickness of the layer varies approximately linearly with the longitudinal distance. For laminar boundary layers, a step length proportional to the square of the layer thickness would be more appropriate.

In some situations, the growth of the layer thickness is very slow, for example in a mixing layer between two streams of nearly equal velocities; in these cases we can choose the step length so that the extra quantity of fluid entrained during that step is equal to a definite fraction of the quantity of fluid already existing in the layer. This rule can be expressed in the following form:

$$\left[\frac{d(\psi_E - \psi_I)}{d\xi_1}\right]_U (\xi_{1,D} - \xi_{1,U}) = \text{const.} \times (\psi_E - \psi_I)_U. \qquad (3.5.2)$$

3.6. *Formula for grid control*

The quantity $(\psi_E - \psi_I)$ appears in all the difference equations given so far. It is therefore necessary to describe the means of calculating $(\psi_E - \psi_I)$ for successive values of ξ_1. It is this quantity that determines the actual size of the grid; the following formulae will therefore be called the grid-control formulae.

It is easy to see that:

$$(\psi_E - \psi_I)_D = (\psi_E - \psi_I)_U + \left[\frac{d(\psi_E - \psi_I)}{d\xi_1}\right]_U \cdot (\xi_{1,D} - \xi_{1,U}), \qquad (3.6.1)$$

where $G-$ denotes the grid point next to G on a constant $-\xi_1$ line, and the subscript $GG-$ boundary happens to be a wall or a line of symmetry, the calculation of the corresponding $d\psi/d\xi_1$ is straightforward, for example by use of equation (2.4.1). We consider below the more important case of a free boundary. Again it is necessary to distinguish between the two sub-classes of this case.

Free-stream boundary with vanishing transport properties. For this case, we write the equation (2.4.3) in finite-difference form as follows:†

$$-\frac{d\psi_G}{d\xi_1} = \frac{1}{(\psi_E - \psi_I)} \frac{(4r^2 l_1 G_1 \mu_{1,\text{eff}})_{GG-}}{|\omega_G - \omega_{G-}|}, \qquad (3.6.2)$$

where $G-$ denotes the grid point nest to G on a constant $-\xi_1$ line, and the subscript $GG-$ indicates evaluation in between the points G and $G-$. The equation (3.6.2) is obtained by assuming ϕ to stand for V_1, and by taking the profile for V_1 as parabolic with distance in the interval between $G-$ and G. It is possible to devise alternative forms.

Free-stream boundary with non-vanishing transport properties. The basis for the grid-control formula for this case has been explained in Section 2.4. In order to present the formula in finite-difference form, we need to re-write the equation (2.1.16) after putting ω equal to zero or unity and by expressing the term

† $\sigma_{\phi,\text{eff}}$ is unity, when V_1 is the property in question; so it does not appear explicitly in the equation.

value ϕ^*; the expression resulting from the flux term will be taken as the same as in equation (3.6.2). Thus we have:

$$-\frac{d\psi_G}{d\xi_1} = \frac{(4r^2 l_1 G_1 \mu_{1,\text{eff}})_{GG-}}{(\psi_E - \psi_I)|\omega_G - \omega_{G-}|} + \frac{\left\{\left(\frac{\Phi l_1}{G_1}\right)_{G_1} - \frac{\phi^* - \phi_{G-}}{\xi_{1,D} - \xi_{1,U}}\right\}(\psi_E - \psi_I)}{2(\phi_G - \phi^*)/(\omega_G - \omega_{G-})}. \quad (3.6.3)$$

Here the $\phi \sim \omega$ profile in the interval $GG-$ is assumed to be parabolic for the purpose of calculating $(\partial\phi/\partial\omega)$.

Instability in grid control. We have used an implicit scheme for formulating the difference equations and therefore can confidently expect stability. The equation (3.6.1) for calculating $(\psi_E - \psi_I)$, however, is of the explicit type; i.e. the upstream value of the derivative $d(\psi_E - \psi_I)/d\xi_1$ is used for the whole interval. This can give rise to fluctuations in the value of the thickness of the layer, when large steps in the ξ_1 direction are used. One way to avoid these fluctuations is to use a weighted mean of the current value of the derivative and that for the previous integration. The fluctuations of the boundary are more likely to arise when the velocity in the surrounding stream is zero. This is to be expected because then if the entrainment rate happens to be rather large, the boundary has to be shifted by a very large distance to entrain the extra quantity of fluid. Use of a small but finite value of velocity in the surrounding stream will restore stability. Finally, if the size of the forward step is reasonably small, instability through grid control will not normally arise.

It should be noted that the grid-control procedure is the part of the present calculation method that most needs ingenuity and care. It would be desirable in the long run to devise a single general procedure which can be applied irrespective of whether or not the transport properties vanish at the boundary.

4. APPLICATIONS

In this section we shall demonstrate the capabilities of the calculation procedure described so far, by way of three examples. The purpose of this section is to show that the present method can be successfully used for predicting heat transfer and friction in various types of flow. Though we shall, of necessity, use physical hypotheses and make comparisons with experimental data, the emphasis is on presenting a convenient mathematical tool and not on demonstrating that the hypotheses which we have used are the best ones.

A remark regarding the change of notation will be helpful here. Having completed the presentation in terms of the general coordinate system, we can now use symbols that are simpler and more familiar. Thus we use below u for V_1, and x and y for distances in direction 1 and direction 2 respectively.

4.1. *Compressible laminar boundary layer on flat plate*

Statement of problem. To test the effectiveness of the new mathematical procedure, comparison with available exact solutions is highly desirable. Therefore, as our first example, we have chosen the flat-plate laminar boundary layer for which Van Driest [12] has presented exact numerical solutions. The problem is characterized by zero pressure gradient, no mass transfer, uniform wall temperature, uniform specific heat, uniform Prandtl number (equal to 0·75), and viscosity variation given by the Sutherland law, namely:

$$\frac{\mu}{\mu_G} = \left(\frac{T}{T_G}\right)^{\frac{1}{2}} \frac{1{\cdot}505}{1 + 0{\cdot}505(T_G/T)}, \quad (4.1.1)$$

where μ and T respectively stand for viscosity and absolute temperature, while the subscript G denotes conditions in the main stream. The ratio of specific heats, γ, is taken as 1·4 and the density is assumed to be inversely proportional to the absolute temperature. The task is to calculate the drag coefficient and the Stanton number for various Mach numbers and for

various wall-to-mainstream temperature ratios.

Details of solution procedure. In this case the partial differential equations solved were (2.1.4) and (2.1.7). The number of grid lines across the layer was 16. The initial profiles of velocity and temperature were arbitrarily taken as linear with distance. The grid-control procedure used was, of course, that for the boundary with non-vanishing viscosity. The value of ϕ^* was taken as 0·999 u_G, where u_G is the free-stream velocity. The integration was continued until the profiles of velocity and temperature ceased to change. In this state the boundary-layer thickness becomes proportional to the square root of the longitudinal distance along the plate. This equilibrium state was achieved after about 150 integration steps and 0·2 min of IBM 7090 computer time.

Results. Figures 6 and 7 respectively show the variations of $\bar{c}_f(\sqrt{Re})$ and $St(\sqrt{Re})$ with Mach number, for various temperature ratios. The full lines represent the solutions from [12] and the points show our solution. The agreement is satisfactory. Thus the present method enables one to obtain accurate solutions of the equations for "similar" boundary layers, even though it is not specifically designed for this purpose.

4.2. *Axisymmetrical turbulent jet*

Statement of problem. As our second example, we take the problem of an axi-symmetrical turbulent jet. Figure 8 shows a jet with velocity

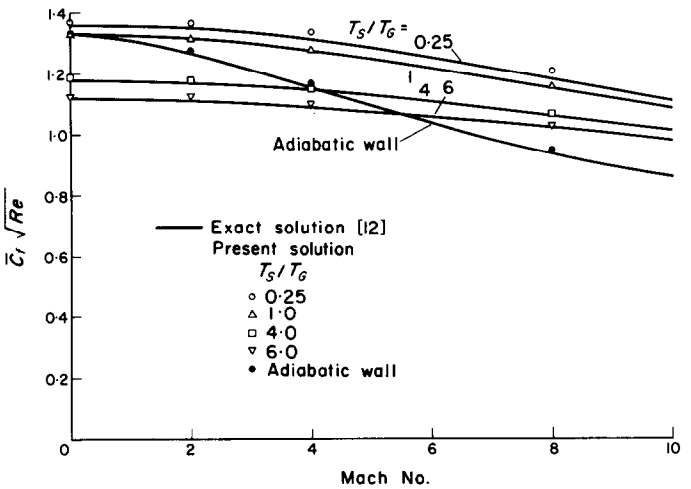

FIG. 6. Variation of mean skin-friction coefficient.

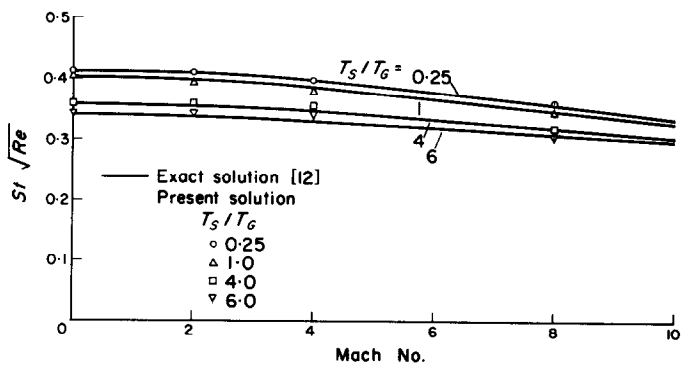

FIG. 7. Variation of Stanton number.

$u_{I,0}$ coming out from a nozzle of diameter d into a surrounding stream of uniform velocity u_E. The density is uniform. The problem is to calculate the centre-line velocity at various downstream distances, the velocity profiles, etc.

Details of solution procedure. For this case the partial differential equation (2.1.4) was solved. The effective viscosity was calculated by using Prandtl's 1925 mixing-length hypothesis, which has been described in Section 2.2. The mixing length was taken as uniform across the layer and equal to 0·0845 times a characteristic thickness of the layer, defined as the distance between two points each of which is near one of the boundaries of the layer; when the boundary coincides with a wall or with a line of symmetry, such a point lies on the boundary; when the boundary is adjacent to a free stream, the point is located such that the velocity there differs from the free-stream velocity by 1 per cent of the maximum velocity difference across the layer.

To start the integration, a linear velocity profile with a very small thickness of the layer was used. The radius of the inner boundary was calculated from the rate of entrainment from the potential core into the inner surface. After the inner radius became zero, the inner boundary was considered to be the line of symmetry. The number of grid lines across the layer was eleven. The forward step was chosen so that the extra amount of fluid entrained during each step was equal to one-tenth of the quantity of the fluid already within the layer.

Results. Figure 9 shows the decay of the centre-line velocity of the jet with downstream distance, for three velocity ratios: $u_E/u_{I,0} = 0$, 0·2, 0·5. Also shown is the line representing the relation:

$$\frac{u_I - u_E}{u_{I,0} - u_E} = \frac{6{\cdot}5}{x/d}, \qquad (4.2.1)$$

which is known to agree well with most of the experimental data for the downstream region of free jets in stagnant surroundings. The agreement with equation (4.2.1) of the present solution for $u_E/u_{I,0} = 0$ is quite good.

Each curve on Fig. 9 represents about 0·25 min of IBM 7090 computer time.

For the downstream region of a jet in stagnant surroundings, Tollmien [13] has obtained an

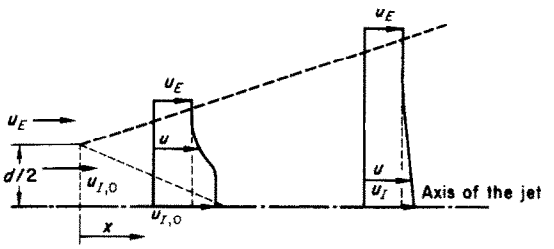

FIG. 8. The axi-symmetrical jet.

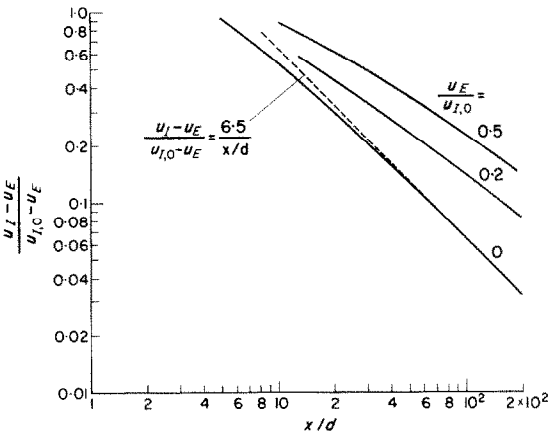

FIG. 9. Decay of centre-line velocity of the jet.

so that the extra amount of fluid entrained exact solution for the Prandtl 1925 mixing-length hypothesis. As a mathematical test of our procedure, we should expect good agreement between the present solution and Tollmien's solution. In Fig. 10 is presented the comparison of the dimensionless velocity profiles. We can conclude that use of only eleven grid lines has predicted very satisfactory velocity profiles.

4.3. *Radial wall jet*

Statement of the problem. As a final illustration, we present the results of a calculation of a

radial wall jet. Though it is within the scope of boundary-layer theory, this case has several unusual features: the flow direction is at right angles to the axis of symmetry (i.e. $\beta = 90°$); the flow contains characteristics of both the conventional boundary layer and the free jet;

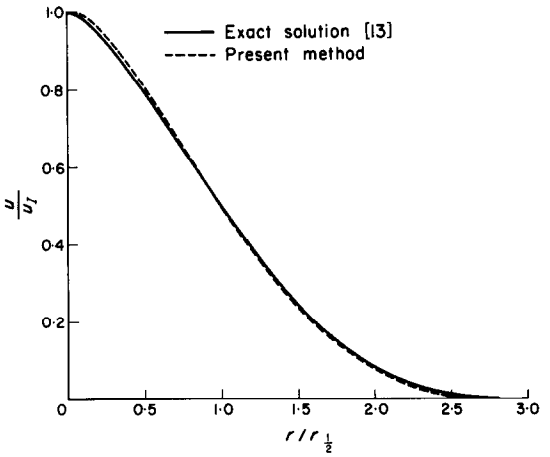

FIG. 10. Dimensionless velocity profile in the jet: comparison of the present and exact solutions.

the velocity profiles exhibit a maximum, and consequently the shear stress changes sign. In practice, such a flow occurs when a jet impinges normally on a plate. The problem here is to predict the development of the velocity profile for such a wall jet on smooth wall, starting from a known velocity profile at a given distance from the axis of symmetry.

Details of solution procedure. Once again the partial differential equation solved was (2.1.4). The effective viscosity was calculated by using Prandtl's 1925 mixing-length hypothesis. The variation of mixing length l_m was taken as:

$$\left.\begin{aligned} 0 < y \leqslant \frac{\lambda_G y_l}{\kappa}: \quad & l_m = \kappa y; \\ \frac{\lambda_G y_l}{\kappa} \leqslant y: \quad & l_m = \lambda_G y_l; \end{aligned}\right\} \tag{4.3.1}$$

where y_l is the characteristic thickness defined in Section 4.2 and κ and λ_G are constants. We have used: $\kappa = 0{\cdot}5$, and $\lambda_G = 0{\cdot}12$. These values will appear to be somewhat higher than those appropriate to conventional boundary layers or plane wall jets. However, experimental data for entrainment and shear stresses in *radial* wall jets do show that the corresponding mixing length must be larger.

For the first interval near the wall, we have assumed that the velocity profile corresponds to the "universal" law of the wall, given by:

$$u^+ = \frac{1}{\kappa} \ln (9y^+). \tag{4.3.2}$$

The shear stress at the wall can be calculated from this law, which incidentally is an example of the Couette-flow relationships mentioned in Section 2.3.

The number of grid lines used across the layer was sixteen and forward steps of one-fourth of the layer thickness were taken.

The calculations were performed for a particular set of experimental data taken from [14].

Results and comparison with experiment. Figure 11 shows our predictions and the experimental data for the decay of maximum velocity

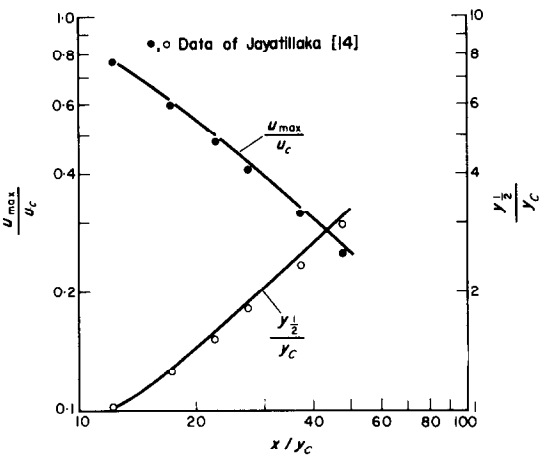

FIG. 11. Decay of maximum velocity and growth of half-value thickness of a wall jet.

and for the growth of the half-value thickness $y_{\frac{1}{2}}$. This half-value thickness is defined as the distance from the wall of a point which is beyond the maximum and at which the velocity

is equal to one-half of the maximum velocity. The symbols y_C and u_C stand respectively for the thickness of the slot and the velocity at it in the experimental situation under consideration. The distance x is measured from the slot. The agreement with experiment is satisfactory in this case. Indeed the constants κ and λ_G have been chosen so as to obtain good agreement.

The integration takes about 0·2 min of IBM 7090 computer time.

5. CONCLUSIONS

1. The foregoing method of solving sets of simultaneous non-linear parabolic differential equations has proved itself to be convenient, accurate and quick in three rather different circumstances.
2. The main merits of the method derive from its use of the non-dimensional stream function as cross-stream variable and of a grid-control procedure ("entrainment law") which locally satisfies the differential equation of motion. Other features of the method, for example the linearisation of the finite-difference formulae, are inessential, and perhaps not particularly worthy of emulation.
3. Considerable simplification has been effected, for turbulent flows, by the neglect of longitudinal convection in the interval close to the wall; this permits the momentum and heat flux through the laminar sub-layer to be expressed by algebraic relations based upon once-for-all integrations or empirical laws.
4. Further development of the method should be directed towards the formulation of a general, optimum entrainment law, and the testing of the procedure for confined flows.

ACKNOWLEDGEMENTS

A part of the development of the method was carried out by the authors at Northern Research and Engineering Corporation, Cambridge (Massachusetts). Thanks are also due to Mr. P. Dale, of Imperial College, for assistance in some of the computation work.

REFERENCES

1. S. V. PATANKAR and D. B. SPALDING, A calculation procedure for heat transfer by forced convection through two-dimensional uniform-property turbulent boundary layers on smooth impermeable walls, in *Proceedings of 3rd International Heat Transfer Conference*, Chicago 1966, Vol. II, p. 50.
2. L. BINDER, *Doctoral dissertation of the Technische Hochschule, München.* Knapp, Halle (1911); and E. SCHMIDT, *Föppl's Festschrift*, p. 179. Springer, Berlin (1924).
3. J. CRANK and P. NICHOLSON, A practical method for numerical evaluation of solutions of partial differential equations of the heat-conduction type, *Proc. Camb. Phil. Soc. Math. Phys. Sci.* **43**, 50 (1947).
4. V. M. PASKONOV, A standard programme for the solution of boundary-layer problems, in *Numerical Methods in Gas Dynamics*, edited by G. E. ROSLYAKOV and L. A. CHUDOV, pp. 74–79, NASA, Washington TTF-300, TT65-50138 (1966).
5. L. PRANDTL, Bericht über Untersuchungen zur ausgebildeten Turbulenz, *Z. Angew. Math. Mech.* **5**(2), 136–139 (1925).
6. A. N. KOLMOGOROV, Equations of the turbulent motion of an incompressible fluid, *Izv. Akad. Nauk SSSR Ser. Phys.* **6**(1/2), 56–58 (1942).
7. L. PRANDTL, Über ein neues Formelsystem für die ausgebildete Turbulenz, Nachrichten der Akad. Wiss. Gottingen, Math. Phys, 6 (1945).
8. A. S. MONIN, Dynamic turbulence in the atmosphere, *Izv. Akad. Nauk.* **14**(3), 232–254 (1950).
9. G. S. GLUSHKO, Turbulent boundary layer on a flat plate in an incompressible fluid, *Izv. Akad. Nauk SSSR Mekh* (4), 13 (1965).
10. S. V. PATANKAR, Wall-shear-stress and heat-flux laws for the turbulent boundary layer with a pressure gradient, Imperial College, London, Department of Mechanical Engineering Tech. Note TWF/TN/14 (1966).
11. G. N. ABRAMOVICH, *The Theory of Turbulent Jets.* M.I.T. Press, Cambridge, Mass. (1963).
12. E. R. VAN DRIEST, Investigation of laminar boundary layer in compressible fluids using the Crocco method, NACA TN 2597 (1952).
13. W. TOLLMIEN, Berechnung turbulenter Ausbreitungsvorgänge, *Z. Angew. Math. Mech.* **6**, 468–478 (1926); Also translated as NACA TM 1085 (1945).
14. C. L. V. JAYATILLAKA, The influence of Prandtl number and surface roughness on the resistance of the laminar sublayer to momentum and heat transfer, Imperial College, London, Department of Mechanical Engineering, Report TWF/R/2 (1966).

Résumé—Un processus pas à pas, numérique, implicite et général est présenté pour la solution d'équations paraboliques aux dérivées partielles, et plus particulièrement de celles de la couche limite. La principale nouveauté réside dans le choix d'une grille qui ajuste son écartement de façon à s'adapter à l'épaisseur

de la couche limite dans laquelle existent des gradients importants. La fonction de courant sans dimensions est employée comme variable indépendante dans la couche limite.

Les possibilités de la méthode sont montrées en l'appliquant à: la plaque plane chauffée dans un écoulement laminaire à nombre de Mach élevé; le jet turbulent à symétrie de révolution dans une atmosphère en mouvement ou au repos; et le jet pariétal turbulent radial.

Zusammenfassung—Es wird ein allgemeines, implizites, numerisches fortschreitendes Rechenverfahren angegeben, das zur Lösung partieller Differentialgleichungen vom parabolischen Typ, insbesondere der Grenzschichtdifferentialgleichungen, geeignet ist. Das wesentlich Neue an diesem Verfahren liegt in der Wahl eines Differenzengitters, das seine Schnittweite der Dicke der Schicht anpasst in welcher bedeutende Gradienten der Zustandsgrössen auftreten.

Die dimensionslose Stromfunktion dient als unabhängige Variable über die Grenzschicht.

Die Leistungsfähigkeit der Methode wird durch Anwendung auf folgende Probleme gezeigt: beheizte ebene Platte mit einer Laminarströmung hoher Mach-Zahl; axial symmetrischer turbulenter Freistrahl in bewegter und ruhender Umgebung; und radial turbulenter Wandstrahl.

Аннотация—Приводится численный метод решения дифференциальных уравнений параболического типа в частных производных применительно к задачам пограничного слоя. Новизна, в основном, относится к выбору сетки, ширина которой соответствует толщине слоя, в котором имеются значительные градиенты основных параметров.

Безразмерная функция тока используется в качестве независимой переменной поперек слоя. Возможности метода иллюстрируются следующими примерами: нагретая плоская пластина в ламинарном потоке при больших числах Маха; осесимметричная турбулентная струя в движущейся и неподвицной средах; радиальная турбулентная пристенная струя.